AFRL-AFOSR-JP-TR-2019-0016

Hierarchical Interaction of Polymer Crystals on Two Dimensional Transition Metal Dichalogenide Nanosheets

Cheolmin Park
YONSEI UNIVERSITY UNIVERSITY-INDUSTRY FOUNDATION

02/28/2019
Final Report

DISTRIBUTION A: Distribution approved for public release.

Air Force Research Laboratory
AF Office Of Scientific Research (AFOSR)/ IOA
Arlington, Virginia 22203
Air Force Materiel Command

REPORT DOCUMENTATION PAGE

Form Approved
OMB No. 0704-0188

The public reporting burden for this collection of information is estimated to average 1 hour per response, including the time for reviewing instructions, searching existing data sources, gathering and maintaining the data needed, and completing and reviewing the collection of information. Send comments regarding this burden estimate or any other aspect of this collection of information, including suggestions for reducing the burden, to Department of Defense, Executive Services, Directorate (0704-0188). Respondents should be aware that notwithstanding any other provision of law, no person shall be subject to any penalty for failing to comply with a collection of information if it does not display a currently valid OMB control number.
PLEASE DO NOT RETURN YOUR FORM TO THE ABOVE ORGANIZATION.

1. REPORT DATE *(DD-MM-YYYY)*	2. REPORT TYPE	3. DATES COVERED *(From - To)*
15-03-2019	Final	19 Aug 2016 to 18 Aug 2018

4. TITLE AND SUBTITLE
Hierarchical Interaction of Polymer Crystals on Two Dimensional Transition Metal Dichalogenide Nanosheets

5a. CONTRACT NUMBER

5b. GRANT NUMBER
FA2386-16-1-4058

5c. PROGRAM ELEMENT NUMBER
61102F

6. AUTHOR(S)
Cheolmin Park

5d. PROJECT NUMBER

5e. TASK NUMBER

5f. WORK UNIT NUMBER

7. PERFORMING ORGANIZATION NAME(S) AND ADDRESS(ES)
YONSEI UNIVERSITY UNIVERSITY-INDUSTRY FOUNDATION
50 Yonsei-ro, Seodaemun-g
SEOUL, 120-749 KR

8. PERFORMING ORGANIZATION REPORT NUMBER

9. SPONSORING/MONITORING AGENCY NAME(S) AND ADDRESS(ES)
AOARD
UNIT 45002
APO AP 96338-5002

10. SPONSOR/MONITOR'S ACRONYM(S)
AFRL/AFOSR IOA

11. SPONSOR/MONITOR'S REPORT NUMBER(S)
AFRL-AFOSR-JP-TR-2019-0016

12. DISTRIBUTION/AVAILABILITY STATEMENT
A DISTRIBUTION UNLIMITED: PB Public Release

13. SUPPLEMENTARY NOTES

14. ABSTRACT
The PI has sucessfully completed the objectives of the grant. The aim is to study the multi-scale structural self-assembled interactions of polymers on transition metal dichalcogenides (TMDs), single crystalline organics based on the comprehensive understanding of molecule-to-molecule and crystal lattice-to-lattice interaction between polymer crystals with hierarchical structures and single or polycrystalline TMDs and organic crystals. The PI was able to understand the molecule to molecule and crytstal lattice to lattice interaction. They were also able to demonstrate a supramolecular assembly route for fabricating cyllindrical nanostrcutures. The PI had 3 peer reviewed journal articles as a direct result of the grant.

15. SUBJECT TERMS
2D Materials, Transition Metal Dichalcongenides, Epitaxy, Polymer Crystals, Nanocomposites, Interface, Nanostructures

16. SECURITY CLASSIFICATION OF:			17. LIMITATION OF ABSTRACT	18. NUMBER OF PAGES	19a. NAME OF RESPONSIBLE PERSON
a. REPORT	b. ABSTRACT	c. THIS PAGE			CHEN, JERMONT
Unclassified	Unclassified	Unclassified	SAR		19b. TELEPHONE NUMBER *(Include area code)* 315-227-7007

Final Report for AOARD Award FA2386-16-1-4058
"Hierarchical Interaction of Polymer Crystals on Two Dimensional Transition Metal Dichalogenide Nanosheets"

18 AUG 2018

<PI and Co-PI information>
Prof. Cheolmin Park
Department of Materials Science & Engineering, Yonsei university
50 Yonsei-ro, Seodaemun-gu, Seoul 03722, Korea
Tel:+82-2-212-2833
Fax:+82-2-312-5375
E-mail: cmpark@yonsei.ac.kr

<Period of Performance>: AUG/19/2017 – AUG/18/2018

1. Abstract

This proposal aims to investigate the multi-scale structural interactions of polymers on transition metal dichalcogenides (TMDs), single crystalline organic semiconductors and thus understand molecule-to-molecule and crystal lattice-to-lattice interaction between polymer crystals with hierarchical structures and single or polycrystalline TMDs and organic crystals for further controlling resulting nanostructures of polymer crystals for potential photo-electric applications. First of all, crystallization of a polymer on a single crystalline organic semiconductor, Rubrene was systematically investigated as a function of a variety of controlling factors such as crystallization rate and thickness of the polymer. The results demonstrate that the characteristic crystal-to-crystal interaction was developed between a host organic single crystal and a guest crystalline polymer, resulting in an intriguing nanostructures where highly aligned polymer lamellae were achieved. The epitaxy of polymer crystals was extended onto a variety of crystals including graphene and TMD and the results clearly show that crystal-to-crystal interaction occurred on all of the surfaces, giving rise to polymer crystals globally ordered with the specific crystal orientations dictated by the epitaxial relation between polymer and a host crystal. We also investigated the supramolecular assembly of end-functionalized polymers, in particular, with pre-patterned guidance for developing globally controlled polymer nanostructures. The study enables us to develop functional periodic nano and micron-scale structures of the polymer crystals which will allow us to extensively characterize their photo-electric properties and thus make them suitable for high performance applications. Vertical-type p-n photodetectors with self-assembled TMD nanosheets were fabricated with excellent photo-switching behavior.

2. Introduction

Objectives: The aim of the 2nd year research of the project is to study the multi-scale structural self-assembled interactions of polymers on transition metal dichalcogenides (TMDs), single crystalline organics based on the comprehensive understanding of molecule-to-molecule and

crystal lattice-to-lattice interaction between polymer crystals with hierarchical structures and single or polycrystalline TMDs and organic crystals and thus to develop intriguing periodic nano and micron-scale structures of the polymer crystals suitable for high performance photo-electric applications of TMD/polymer nanocomposites.

Research Focus: Full realization of the properties of TMDs requires the comprehensive understanding of interface between polymer and TMD and, moreover, to design the interface which would enhance the TMD properties. Both the molecule-to-molecule and crystal-to-crystal interaction between polymer and TMD are examined with chemically designed polymers and crystalline polymers, respectively. Efforts are made to reveal how the controlled molecular structure of a polymer can affect the dispersion of TMDs in liquid phase. In addition, the study focuses on understanding how molecularly ordered polymer crystals are developed on crystalline surface, arising from the crystal-to-crystal epitaxy.

3. Experiment

3-1) Epitaxially Grown Ferroelectric PVDF-TrFE Film on Shape-Tailored Semiconducting Rubrene Single Crystal

Growth of Rubrene

Rubrene single crystals were grown via the PVD method as previously reported. Accordingly, 2 mg of sublimed rubrene powder (>99.5%) was placed in a hot zone of a quartz tube. The source-carrying jar was placed in the crystallization zone (280 °C). Further, 50 sccm of argon (99.999%) was used as the carrier gas. After 5 min of prepurging, the system was heated to 320 °C. The reaction was performed for 5 min and the system was thereafter cooled down to room temperature.

Epitaxy of PVDF-TrFE

PVDF-TrFE copolymer (Mw = 400,000 g mol^{-1}) with 25% mol fraction of TrFE was purchased from Solvay. The melting (Tm) and Curie (Tc) temperatures of PVDF-TrFE were 156 and 80 °C, respectively. A thin film was formed via spin coating of 3–5 wt% solution in methyl ethyl ketone at 1500 rpm for 60 s. An epitaxial PVDF- TrFE was realized when the film was subsequently melted and recrystallized at 200 °C for 30 min on the rubrene surface. The films were heat-treated on the heating stage (Linkam 600, UK) at 200 °C for 30 min.

Microstructure Characterization

An optical microscope (OM) (Olympus BX 51M) was used to visualize the single-crystalline rubrene and devices. The microstructures of the epitaxially grown PVDF- TrFE thin films were characterized using field- emission scanning electron microscopy (JEOL-SM 6701F) with an acceleration voltage of 10 kV. Tapping mode atomic force microscopy (TM-AFM) was performed in the height contrast mode using a Digital instrument Nanoscope 3100 microscope. 2D-GIXD experiments were performed at the Pohang Accelerator Laboratory in South Korea.

3-2) Surface functionalized nanostructures via position registered supramolecular

DISTRIBUTION A: Approved for public release; distribution unlimited

polymer assembly

Materials

Four different endfunctionalized PS or PBD polymers, namely a mono-end-sulfonated polystyrene (SPS) (molecular weight (Mw) = 10.5 kg mol^{-1}, polydispersity index (PDI) = 1.12), a mono-endaminated polybutadiene (APBD) (Mw = 29 kg mol^{-1}, PDI = 1.08), a mono-end-minated polystyrene (APS) (Mw = 9.5 kg mol^{-1}, PDI = 1.10), and a mono-end-aminated polybutadiene (SPBD) (Mw = 19 kg mol^{-1}, PDI = 1.10), were purchased from Polymer Source, Inc. (Doval, Canada). Poly(2-vinyl pyridine) (P2VP) (Mw = 12 kg mol^{-1}, PDI = 1.18) was also purchased from Polymer Source, Inc. PS homopolymer (Mw = 10 kg mol^{-1}, PDI = 1.11) was purchased from Sigma Aldrich Korea (Seoul, Korea). THF, MEK, OsO_4, $HAuCl_4$, coumarin 343, and rhodamine 6G dye were also purchased from Sigma Aldrich Korea. Benzene and HCl were purchased from Daejung (Korea). All chemicals were used as received.

Film preparation

Two different blend solutions of SPS/APBD and APS/SPBD, referred to as supra 1 and supra 2, respectively, were prepared in THF and stirred at 50 °C for 1 day. Subsequent spin-coating (SPIN 1200 Midas-system, Korea) of the solutions with a polymer concentration of 0.8 wt% at a spin rate of 4000 rpm for 60 seconds produced thin supramolecular films with a thickness of ~25 nm on silicon substrates. The films were dried under ambient conditions for 1 day. The graphoepitaxy samples were prepared similarly, but spin-coated on topographically pre-patterned Si substrates with various shapes and sizes.

Solvent annealing

Both supra 1 and supra 2 films were placed in a chamber containing benzene for various time periods ranging from 5 to 30 minutes. The environment outside the chamber was maintained at 20 °C with a humidity of ~20%. The films were removed from the chamber when the residual solvent vapor had completely evaporated through small holes in the chamber.

Selective cross-linking and soft etching

In order to fabricate cylindrical nanopores with either sulfonate or amine surface functionality, thin supramolecularly assembled films were placed in a chamber containing a 2 wt% OsO_4 aqueous solution for 2 minutes. OsO_4 was utilized for preferentially cross-linking PBD. Subsequently, OsO_4-treated films were immersed in a mixture of MEK and HCl for 5 minutes to remove end-functionalized PS. HCl was added to weaken the ionic bonding between the sulfonic acid and amine groups. Cylindrical posts with either sulfonate or amine surface functionality were fabricated by exposing the thin supramolecularly assembled films to UV for

DISTRIBUTION A: Approved for public release; distribution unlimited

1 hour to preferentially cross-link PS. The UV-treated films were subsequently immersed in a MEK/HCl solvent mixture for 5 minutes to remove end-functionalized PBD.

Surface functionality of the nanoporous template

Supra 2 films with vertically ordered cylindrical holes with sulfonic acid groups on their surfaces were immersed for 5 hours in a P2VP solution, when the pyridine groups in the P2VP chains preferentially interacted with the sulfonic acid groups on the pore surface, resulting in nanostructures filled with P2VP after drying under ambient condition for 1 day. The P2VP-modified film was immersed in an aqueous solution containing 1 mM $HAuCl_4$, and subjected to oxygen plasma treatment with 100 W for 10 minutes not only to reduce Au3+ to Au but also to etch the polymer template. The chemically etched supramolecularly assembled films were immersed in a 0.5 wt% aqueous solution of either rhodamine 6G or coumarin 343 for 30 minutes. The residual dyes were washed off with deionized water.

Prepatterns

Topographic Si prepatterns with periodic lines and square dents were fabricated by the conventional optical lithography technique using 193 nm photoresist and subsequent etching with CF_4 plasma. The line pattern has the width of trench of 220 nm and mesa of 180 or 130 nm, respectively, and the circular pattern consists of the square dents of 200 nm and 500 nm in length arrayed with p4mm symmetry. The depth of line trenches and circular dents is ~45 nm.

3-3) Flexible Vertical p–n Diode Photodetectors with Thin N-type $MoSe_2$ Films Solution-Processed on Water Surfaces

Exfoliation of $MoSe_2$ with amine-end-functionalized polymers

$MoSe_2$ powders were purchased from Alfa Aesar and Sigma Aldrich. A PS-NH_2 with the molecular weight and polydispersity index of 9500 g mol^{-1} and PDI ~ 1.16, respectively was produced from Polymer Source Inc., Doval, Canada. A PFO (MW: ~ 58200, PDI: ~ 3.7) was purchased from Sigma Aldrich. All of the solvents used in the present work were also purchased from Sigma-Aldrich. All the materials were used as received unless otherwise stated. In a typical procedure, 250.0 mg of bulk $MoSe_2$ powder and 25.0 mg of PS-NH_2 were added into a 30.0-mL glass vial containing 25.0 mL of toluene. The solution was sonicated for 45.0 min using a tip sonicator with a 10.0-s ON pulse and a 5.0-s OFF pulse at amplitude of 50% in an ice bath. The dispersions were allowed to settle for 24.0 h, and the top dispersion was subsequently decanted and centrifuged for 30.0 min at 1500.0 rpm to remove unexfoliated and large particles. After centrifugation, the top half of the dispersion was collected, and the

DISTRIBUTION A: Approved for public release; distribution unlimited

concentration of $MoSe_2$ nanosheets was determined by standard gravimetric analysis.

4. Results and Discussion

4-1) Epitaxially Grown Ferroelectric PVDF-TrFE Film on Shape-Tailored Semiconducting Rubrene Single Crystal

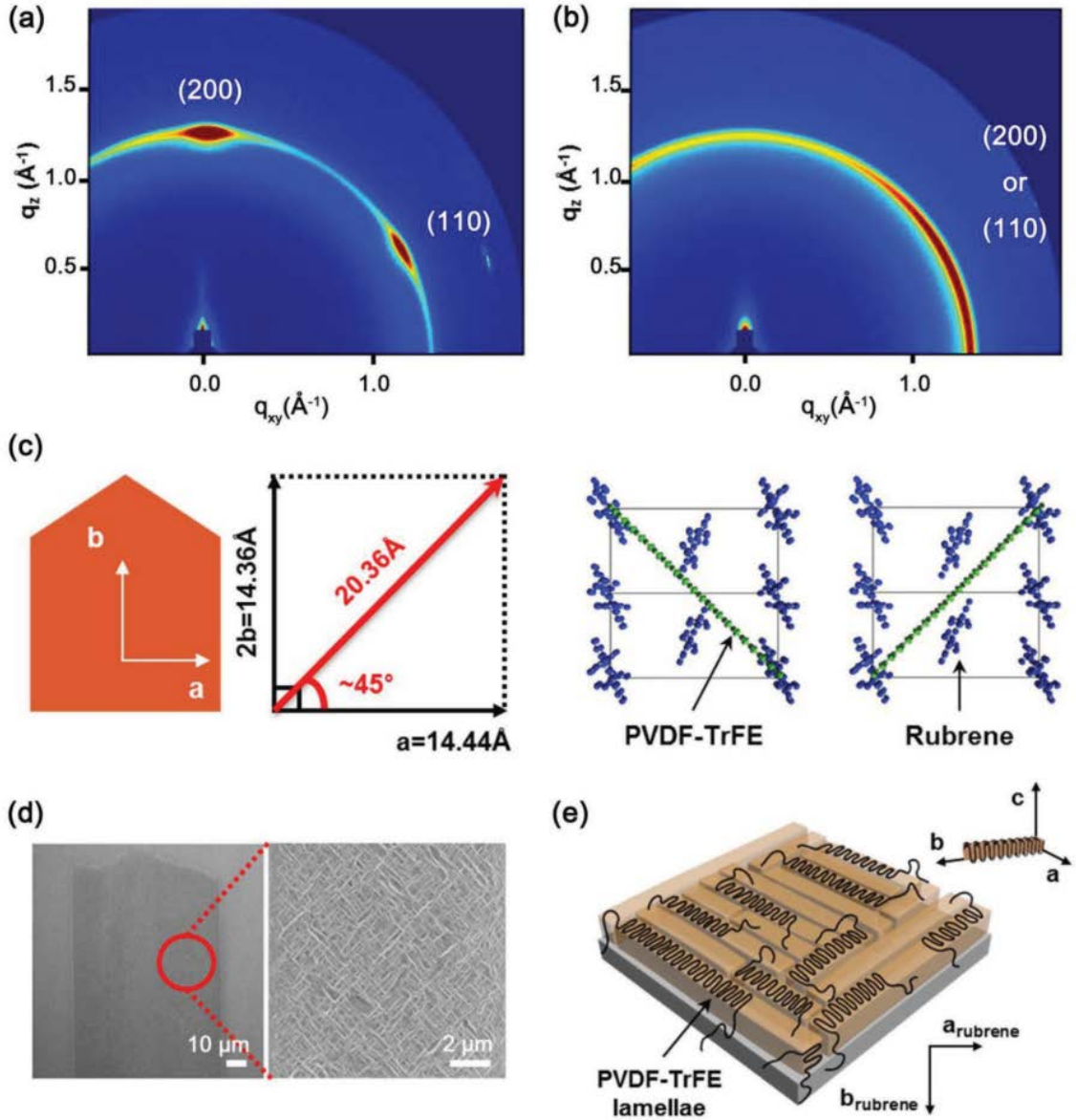

Figure 1. 2D-GIXD patterns of 5 wt% PVDF-TrFE thin films on a) rubrene single crystal and b) SiO2 substrates after thermal annealing at 200 °C for 30 min. Two strong reflections were observed in the film on a rubrene layer in (a), thus presenting the interaction between the PVDF-TrFE crystal and the rubrene layer. c) Schematic illustration of the crystal structure of rubrene and the possible orientation of PVDF-TrFE thin film epitaxially grown on the rubrene surface. Two degenerated crystal orientations are shown with PVDF-TrFE chains aligned along the (210) and (210) planes of orthorhombic rubrene crystal. d) SEM images of the ab-plane of rubrene and magnified image of 45°-aligned PVDF-TrFE lamellae to the b-axis of rubrene single crystal. e) Schematic representation of the microstructural orientation of PVDF-TrFE thin film on the rubrene surface.

DISTRIBUTION A: Approved for public release; distribution unlimited

Rubrene single crystals were grown in a quartz tube by physical vapor deposition (PVD) and subsequently transferred onto the highly doped Si substrate, using a static gun. Grazing incident X-ray diffraction (GIXD) experiments were performed to reveal the molecular orientation of the PVDF-TrFE crystals developed on the rubrene surface. A thin PVDF-TrFE film, melted at 200 °C and subsequently recrystallized on the rubrene surface, exhibits two distinguishable reflection peaks in the 2D-GIXD pattern (Figure 1a). The reflections presumably correspond to the (110) and (200) planes of the PVDF-TrFE crystals appearing at the meridian and the region ≈60° apart from the meridian, respectively. The GIXD results suggest that the c-axis of the PVDF-TrFE crystals is preferentially aligned perpendicular to the rubrene surface normal. However, a thin PVDF-TrFE film molten and recrystallized on an SiO2 substrate exhibits a strong but broad reflection near the equator of a 2D-GIXD pattern, as shown in Figure 1b. The reflection corresponds to either the (110) or (200) plane of the crystal owing to the preferential align- ment of the c-axis, chain axis of PVDF-TrFE parallel to the surface normal.

Considering the crystal lattices of both PVDF-TrFE (unit cell parameters: a = 9.12 Å, b = 5.25 Å, c = 2.55 Å, and β = 93°) and orthorhombic rubrene (unit cell parameters: a = 14.44 Å, b = 7.18 Å, c = 26.97 Å, and α = β = γ = 90°), we could propose a possible epitaxial relation in which the c-axis of PVDF-TrFE unit cell (2.55 Å) was comparable to the (210) plane of the orthorhombic rubrene, as shown in Figure 1c. The comparison between the crystallographic lattices of the two contact planes suggests a possible epitaxy of PVDF-TrFE on both the (210) and (210) planes of orthorhombic rubrene owing to the matching of the PVDF-TrFE inter-chain distance of the c-periodicity (8 times of c-axis of PVDF- TrFE ≈ (210) plane of rubrene) with the lattice mismatching of 0.196%. It has been confirmed that such a checkerboard-shaped polymeric epitaxy can always be obtained at ≈45° to the longitudinal direction of rubrene crystal corresponding to the b-direction, as shown in Figure 1d. Based on the diffraction patterns and molecular results with the proposed epitaxial relation, we suggest that the PVDF-TrFE crystals were preferentially oriented to the rubrene surface, as schematically illustrated in Figure 1e.

DISTRIBUTION A: Approved for public release; distribution unlimited

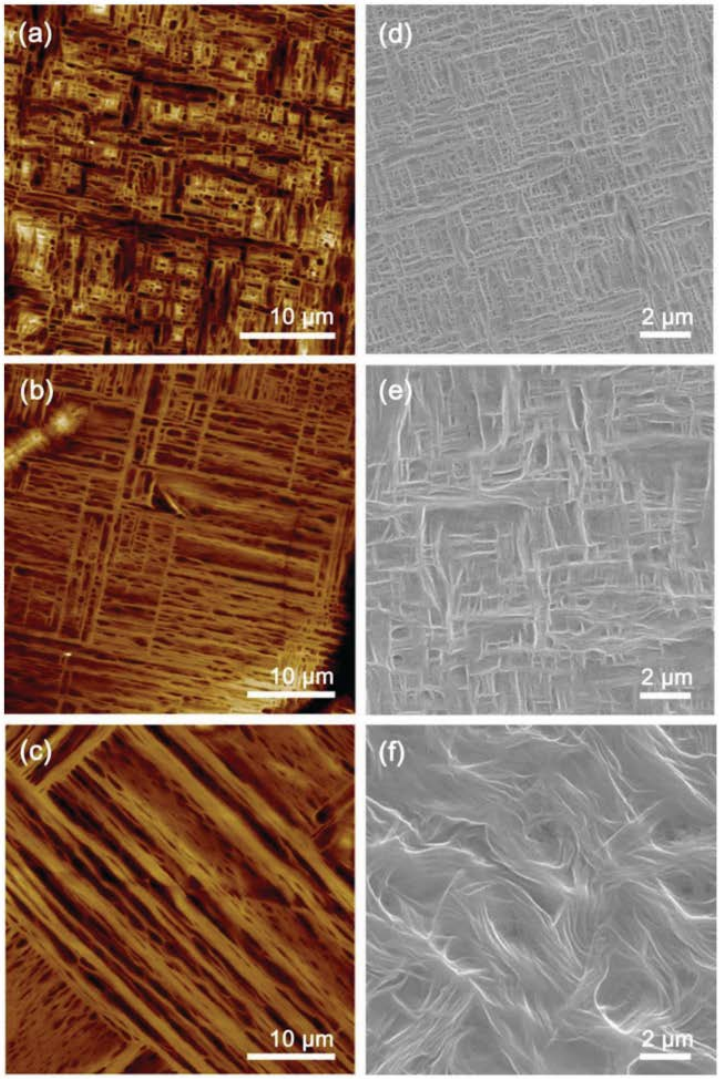

Figure 2. a–c) Tapping mode AFM images in height contrast of epitaxially grown 5 wt% PVDF- TrFE on rubrene single crystal after thermal treatment with different cooling rates during the recrystallization process. After the melting state, the films were recrystallized at the cooling rates of (a) 5 °C min−1, (b) 0.5 °C min−1, and c) 0.1 °C min−1. The slower the cooling rate, the larger the growth of the PVDF-TrFE crystal. d–f) A series of SEM images of PVDF-TrFE films on the rubrene single crystal after thermal annealing, in accordance with the different thicknesses of polymer film. The solution concentration of polymer was (d) 3 wt%, (e) 7 wt%, and (f) 11 wt%.

The relative population of the two nearly orthogonal edge-on lamellae arising from the epitaxial crystallization of PVDF-TrFE on the rubrene surface was controlled by the cooling rate of a thin film from molten state, as shown in Figure 2a–c. When the film was recrystallized at a cooling rate of 5 °C min^{-1}, both the nearly orthogonal edge-on lamellae appear almost equal in population, and the average length of the lamellae was approximately several hundred nanometers (Figure 2a). One of the two orthogonal lamellae was dominantly developed, in which the average lamellae length was significantly longer than before, when the recrystallization occurred slowly at a cooling rate of 0.5 °C min^{-1}, as shown in Figure 2b. The number of nuclei substantially reduced upon recrystallization at the cooling rate of 0.5 °C min^{-1}, which also provides sufficient time for nuclei to grow before impinging upon each other, resulting in lamellae much longer than those obtained at the cooling rate of 5 °C min^{-1}. When

DISTRIBUTION A: Approved for public release; distribution unlimited

the cooling rate was further decreased to 0.1 °C min^{-1}, highly ordered edge-on lamellae grew into several tens of micrometers, as shown in Figure 2c.

As epitaxy is based on the crystallographic matching of two specific materials, it is interesting to examine the epitaxy of PVDF-TrFE crystals on the rubrene surface as a function of film thickness, and the results are shown in Figure 2d–f. Epitaxially grown edge-on lamellae were clearly observed in the film with thickness less than 600 nm, where edge-on but distorted lamellae in their orientation began to appear. When the film was thicker than 2000 nm, the morphology became similar to that observed on the Si substrate, as shown in Figure 2f.

4-2) Surface functionalized nanostructures via position registered supramolecular polymer assembly

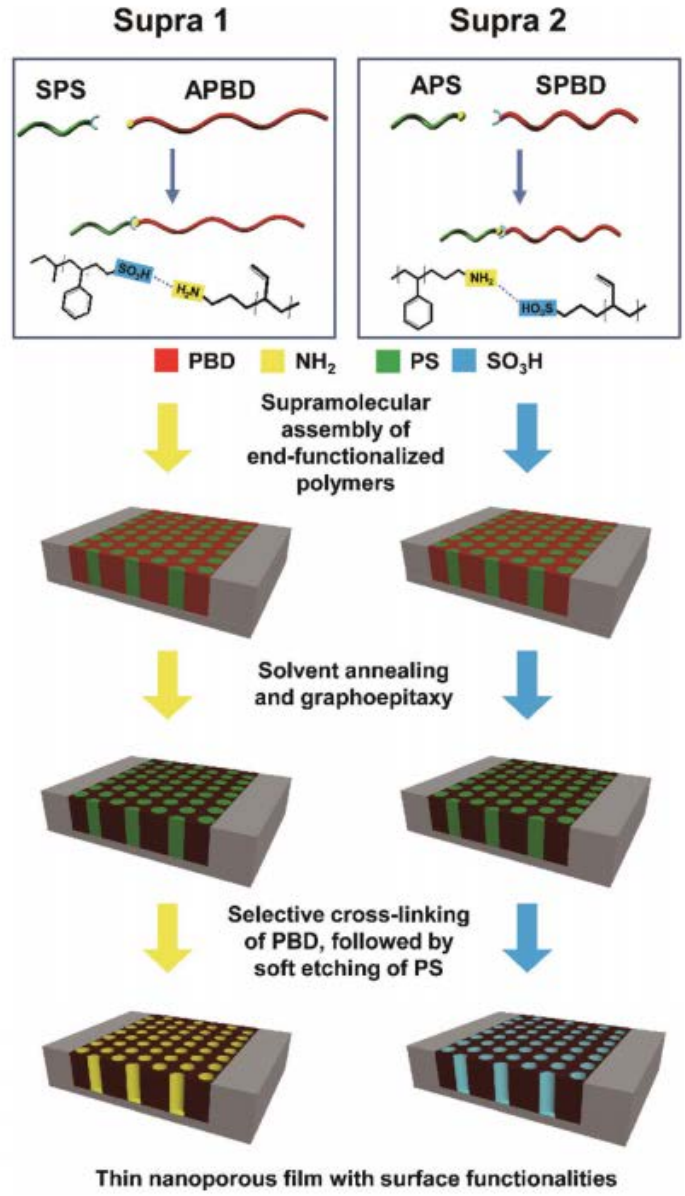

Figure 3. Schematic of the fabrication of supramolecularly assembled nanopores with different surface chemical functionalities confined in the topographically pre-patterned substrates. Two pairs of binary blends are shown of

DISTRIBUTION A: Approved for public release; distribution unlimited

mono-end-functionalized polymers of (supra 1) monoend-sulfonated polystyrene (SPS) and mono-end-aminated poly(butadiene) (APBD) and (supra 2) mono-end-aminated polystyrene (APS) and mono-end-sulfonated poly(butadiene) (SPBD) with two complementarily interacting end-sulfonated and aminated groups. Thin supramolecularly assembled films guided in the pre-patterns were solvent-annealed, followed by chemical etching of end-functionalized PS after the crosslinking end-functionalized PBD, giving rise to globally ordered nanopores with different chemical functionalities.

Surface-functionalized supramolecularly assembled nanostructures

Our method is based on the supramolecular assembly of the polymer pair, SPS and APBD, referred to as supra 1, and APS and SPBD, referred to as supra 2, through ionic bonding between the proton-donating sulfonic acid and the proton-accepting amino groups, as schematically depicted in Figure 3. For the film preparation, a mixture of SPS (10.5 kg mol^{-1}) and APBD (29 kg mol^{-1}) (supra 1) and a mixture of APS (9.5 kg mol^{-1}) and SPBD (19 kg mol^{-1}) (supra 2), both dissolved in tetrahydrofuran (THF), which is a good solvent for the polymers, were spin-coated on Si wafers. Both mixtures were prepared with the stoichiometric SPS weight fraction ΦPS = 0.27 in supra 1 and the APS weight fraction ΦPS = 0.33 in supra 2, using which the number of sulfonic acid groups of one of the polymers were equalized with the number of amino groups of the other, to ensure 1 : 1 association between the two supramolecular polymers. Solvent annealing with benzene vapors was employed to further control the architecture of supramolecularly assembled nanostructures originating from the end-to-end ionic attraction and nonspecific repulsion between the styrene and butadiene monomers, as shown in Figure 3. In contrast with the conventional block copolymer, our supramolecularly assembled nanostructures are beneficial in that the numerous end-functional groups on the surface of the nanostructure can be further utilized after selective chemical etching of one of the polymers, as shown later. To achieve this, either APBD or SPBD in a solvent annealed film was chemically cross-linked, followed by the solvent assisted selective etching of either SPS or APS. Supra 1 and supra 2 produced periodically assembled cylindrical holes with either sulfonate or amino surface functionality, as shown schematically in Figure 3. Furthermore, the orientation of the supramolecularly assembled nanostructures is controlled when the nano-structures are appropriately confined to topographically prepatterned substrates.

DISTRIBUTION A: Approved for public release; distribution unlimited

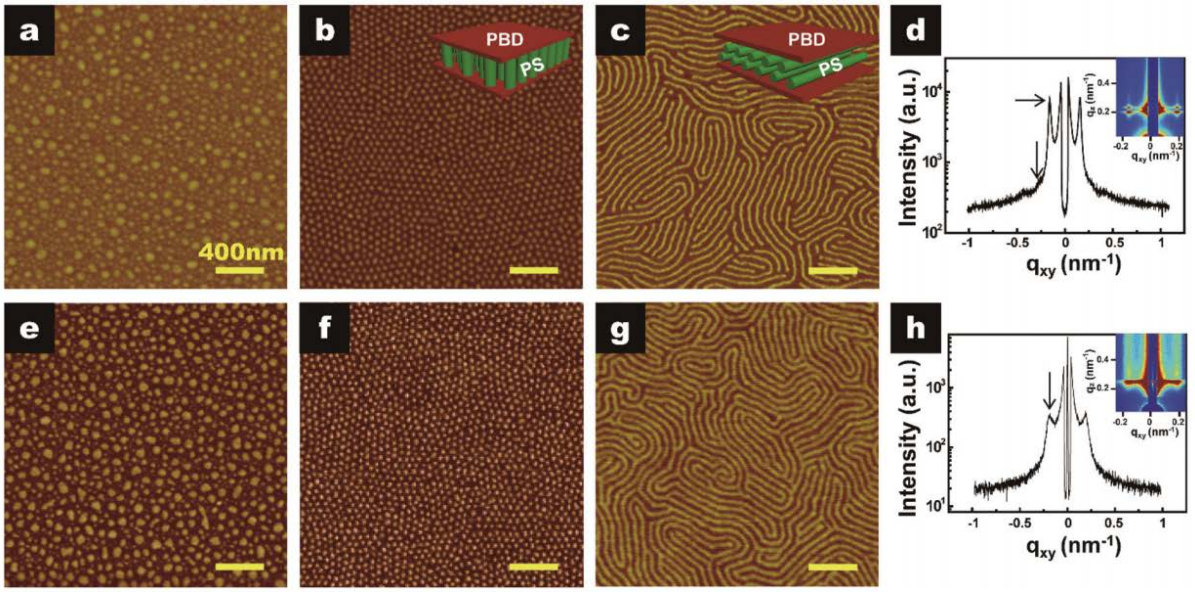

Figure 4. TM-AFM images in phase contrast of supramolecularly assembled nanostructures of supra 1 and 2 films as-cast (a, e) and prepared at different solvent annealing times of 5 (b, f) and 30 min (c, g), respectively. (d, h) One-dimensional GISAXS plots of supra 1 and 2 films after solvent annealing for 5 min, respectively. The inset images correspond to two-dimensional GISAXS patterns.

Supramolecularly assembled nanostructures obtained by solvent annealing.

The supramolecular assembly of our two end-functionalized polymers occurs upon the spincoating process even before the solvent annealing step, giving rise to a characteristic nanostructure whose orientation is, however, hardly controlled. A subsequent solvent annealing provides sufficient chain mobility to the two polymers, rendering the as-cast nanostructure more ordered with its long range orientation. The supramolecularly assembled nanostructures of both supra 1 and supra 2 were investigated as a function of solvent annealing time using tapping-mode atomic force microscopy (TM-AFM) and two-dimensional grazing incidence small X-ray scattering (GISAXS) (Figure 4). A characteristic nanostructure with rather irregular circular domains was found to immediately develop upon spin-coating, in both supra 1 and supra 2, as shown in Figure 4a and e, respectively. Solvent annealing of thin films of both supra 1 and supra 2 with benzene vapors for 5 minutes yielded hexagonally ordered cylinders of ~20 nm diameter aligned parallel to the surface normal, over the entire film, as shown in Figure 4b and f, respectively. When the solvent annealing time is increased, the vertical cylinders were found to have transformed into in-plane cylinders, in both the films of supra 1 and supra 2, as representatively shown in Figure 4c and g, respectively. The polymer blend solutions were prepared with the PS volume fraction of 0.33, which was the same as that used in the supra 2. An as-cast film of the PS/APBD blend clearly shows the morphology where the constituent polymers are macroscopically phase separated due to thermodynamically unfavorable mixing energy. Macroscopic PS domains ranging from 100 nm to 800 nm are embedded in the PBD matrix. This morphology is typically observed in numerous polymer blends. The fast solvent evaporation during spin coating frequently results in a few hundreds of nanometers in size phase-segregated domains with a broad size distribution. Subsequent solvent annealing with benzene vapors for the same conditions as those used in the

DISTRIBUTION A: Approved for public release; distribution unlimited

supramolecular assembly provided sufficient chain mobility for both PS and PBD, allowing further phase-segregation. In consequence, PS domains of approximately 1 μm in diameter are obtained, much larger than those in the as-cast film. As expected, further solvent annealing for 30 minutes made PS domains much larger, giving rise to PS domains larger than 3 μm in diameter were obtained. Similar morphologies were also obtained in a blend film of PS/SPBD, which underwent macroscopic phase separation of the two polymers. These results support that the introduction of small functional groups capable of specific interactions gives rise to a variety of intriguing self-assembled morphologies.

The hexagonally ordered cylindrical nanostructures were further analyzed by GISAXS, which is one of the most reliable nanostructure characterization tools for confirming the locally obtained nanostructures from microscopes in numerous materials including block copolymers, supramolecular assembled polymers and self-assembled surfactants, and the results are shown in Figure 4d and h. The scattering pattern from a thin supra 1 film solvent-annealed for 5 minutes shows strong first order reflection at the in-plane scattering vector, qxy, of ~0.158 nm^{-1} and weak second order reflection is observed at 0.272 nm^{-1}, as shown in Figure 4d. A one-dimensional (1D) plot of the GISAXS results confirms the hexagonal packing of the in-plane cylinders with the relative peak positions of the high-order reflections with respect to the first peak position (qn/q1) yielding the expected values of 1 and $\sqrt{3}$. The (100) plane distance obtained from $2\pi/q1$ is ~40 nm, which agrees well with the results from the AFM analysis (Figure 4b). GISAXS also reveals the hexagonally packed cylindrical structure of the in-plane cylinders when the supra 1 film was solvent-annealed for 30 minutes. The 1D plot of the GISAXS result exhibits the relative scattering peak positions with respect to the first reflection (qn/q1), yielding expected values of $1 : \sqrt{3} : \sqrt{7}$. A GISAXS pattern of a thin supra 2 film (Figure 4h), however, shows only its strong first order reflection at 0.192 nm^{-1}, owing to the lack of long-range ordering of the cylindrical domains.

DISTRIBUTION A: Approved for public release; distribution unlimited

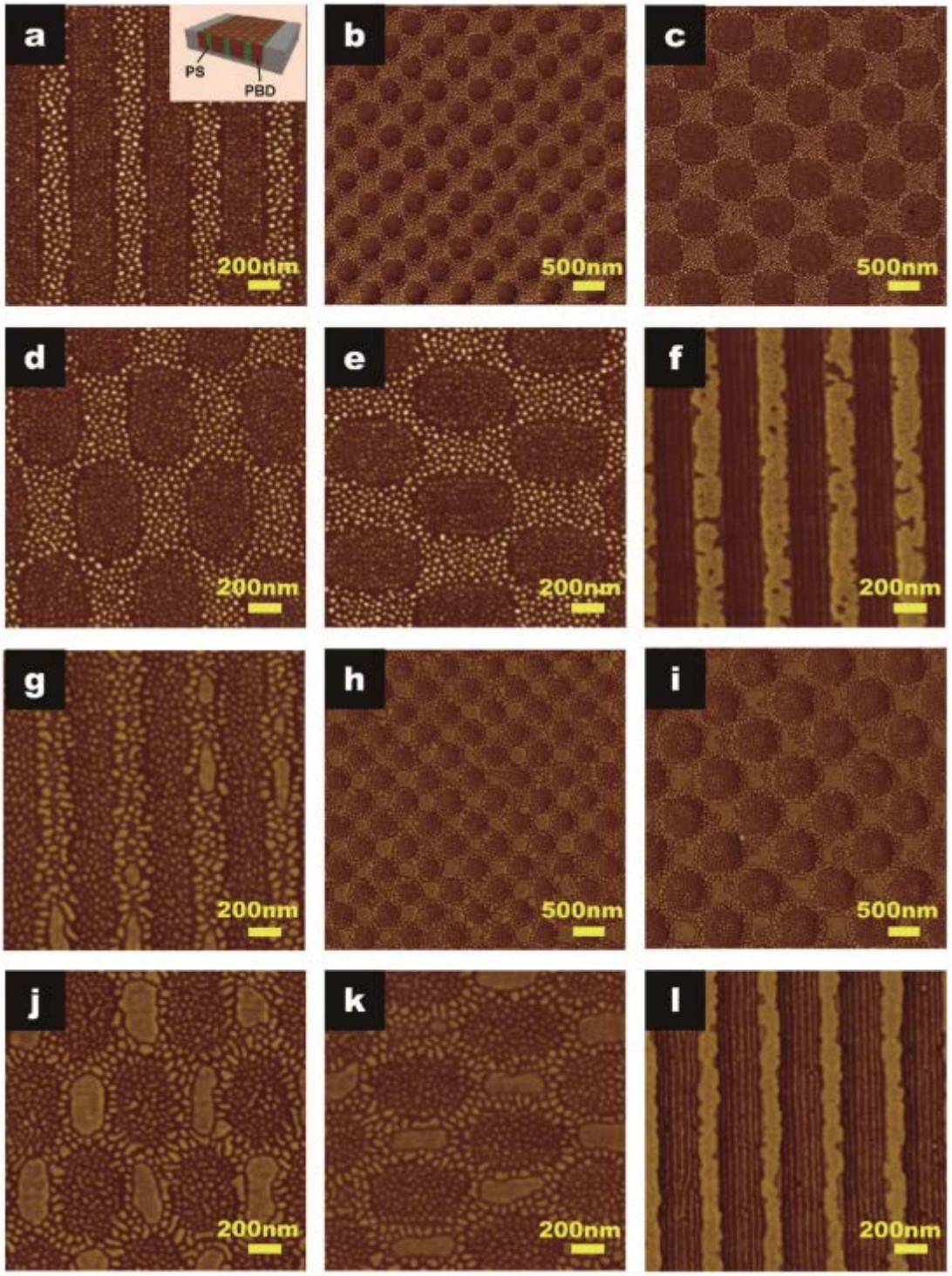

Figure 5. TM-AFM images in phase contrast of the supramolecularly ordered cylindrical nanostructures developed from (a–f) supra 1 and (g–l) supra 2 by solvent annealing confined in topographically pre-patterned substrates. The films were solvent annealed with benzene for (a–e, g–k) 5 and (f, l) 30 min, respectively.

Controlling the supramolecular assembly using topographically patterned substrates

In order to control the orientation of our supramolecular nanostructures from supra 1 and supra 2 over large areas, we employed topographically pre-patterned Si substrates. We envisioned

DISTRIBUTION A: Approved for public release; distribution unlimited

that graphoepitaxy which is well known with conventional block copolymers is also useful for controlling the organization of our supramolecular cylinders. By controlling the solvent annealing time, we were able to efficiently confine both vertical and in-plane cylinders produced from supra 1 assembly to patterns under the same condition, as shown in Figure 5a–f. Control over the cylinders from the assembly of supra 2 was also successfully achieved with various patterns, as shown in Figure 5g–l. The preferential wetting of PBD occurs on the topographically pre-patterned Si substrates and PBD is also present at the polymer/air interface in our supramolecular assembly. For instance, on a substrate with periodic trenches 220 nm in width, 4 and 6 cylinders were confined to an individual trench for supra 1 and supra 2 films, as shown in Figure 5f and l, respectively. The topographically pre-patterned Si substrates affect only the ordering and packing of the resultant supramolecularly assembled nanostructures and there is no difference in the solvent annealing time required to develop nanostructures. We also examined the non-stoichiometric mixtures in the supramolecular blend on the resultant structures in supra 1. As expected, extra end-functionalized polymers not involved in the supramolecular assembly are macroscopically phase-segregated, giving rise to micron-scale domains.

4-3) Flexible Vertical p–n Diode Photodetectors with Thin N-type $MoSe_2$ Films Solution-Processed on Water Surfaces

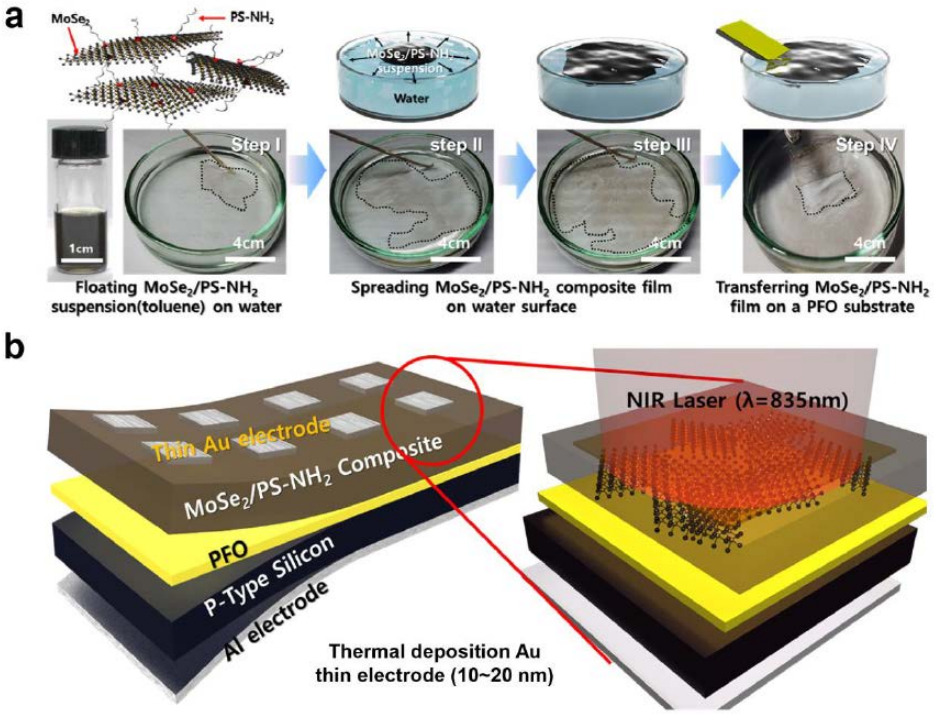

Figure 6. (a) Schematics and photographs illustrating fabrication of a thin $MoSe_2$/PS-NH_2 film at the liquid/air interface. Step I: Preparation of a suspension of $MoSe_2$ nanosheets exfoliated and dispersed with PS-NH_2 in toluene. The schematic shows the nanosheets modified with PS-NH_2 chains via Lewis acid-base interaction between primary amines of PS-NH_2 and Mo atoms. In the step II, droplets of the suspension deposited on water surface uniformly spread with time by Marangoni effect. A thin $MoSe_2$/PS-NH_2 film was developed after complete evaporation of toluene as shown in the step III. The nanocomposite film was readily transferred on a substrate (Step IV). Dotted lines are added for clarification. (b) Schematic illustration of arrays of p-n vertical

diode PDs. The zoomed scheme shows an individual PD with PS-NH_2 modified MoSe2 nanosheets evenly distributed in the composite.

Thin polymer composites with highly dispersed $MoSe_2$ nanosheets was prepared by spreading the suspension of $MoSe_2$ nanosheets mixed with amine terminated poly(styrene) ($PSNH_2$) on water surface, as shown schematically in **Figure 6a.** Efficient exfoliation and dispersion of $MoSe_2$ nanosheets in toluene was obtained with the use of PS-NH_2 combined with sonication and ultracentrifugation, as described in our previous work. Few-layered $MoSe_2$ nanosheets with PS-NH_2 were successfully stabilized in toluene with a maximum concentration of approximately 0.2 mg mL^{-1}. When several droplets of the suspension were deposited on water surface, they immediately spread on the surface because of the Marangoni effect (surface tension of water and toluene being 73.0 and 28.0 dynes/cm, respectively), giving rise to a thin composite film after evaporation of toluene. Therefore, a solvent with a surface energy lower than that of water should be selected to obtain a good spread. Dispersed TMD solutions were prepared using various solvents and we selected a solvent with good dispersion and low surface tension. The thickness of the nanocomposite films was controlled, from approximately 50.0 to 350.0 nm, by controlling the concentration of suspension. The nanocomposite film with n-type $MoSe_2$ nanosheets on the water surface was mechanically transferred onto a thin p-type PFO film (approximately 100.0 nm thickness), spin coated on a boron doped p-type silicon substrate, as shown schematically in **Figure 6b.** The polymeric p-type layer is advantageous because of its mechanical flexibility as well as firm interface with the n-type $MoSe_2$/polymer nanocomposite.

DISTRIBUTION A: Approved for public release; distribution unlimited

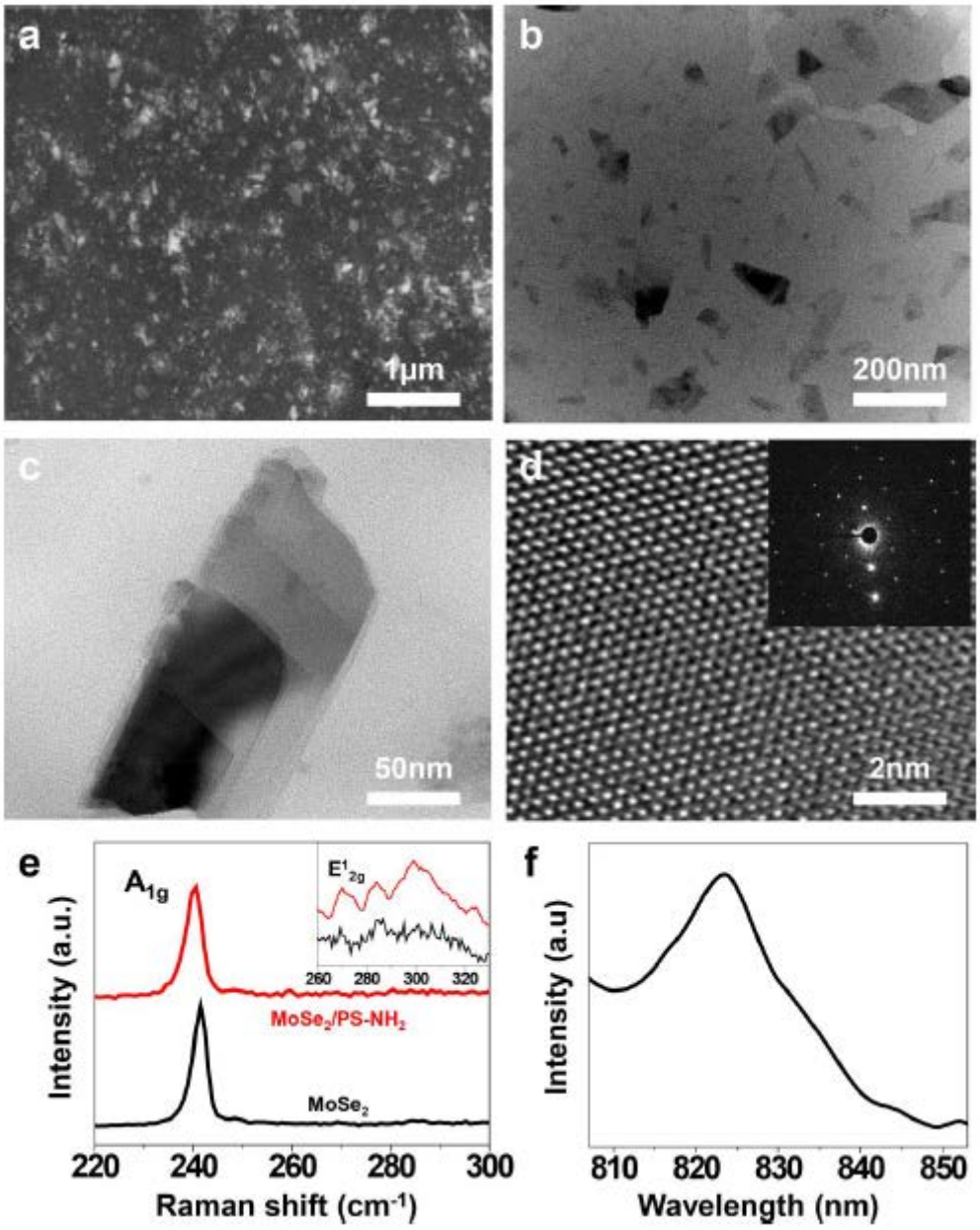

Figure 7. (a) A SEM image of the top view of a thin $MoSe_2$ /PS-NH_2 film. (b) and (c) Bright field TEM images of a thin $MoSe_2$/PS-NH_2 film prepared from a dilute suspension. (d) A HRTEM image of a single-layer $MoSe_2$ nanosheet. The inset shows the Fast Fourier transform (FFT) of the HR-TEM image. (e) A Raman spectrum of a $MoSe_2$ /PS-NH_2 film. A spectrum of bare $MoSe_2$ film is also shown for comparison (black). The inset shows the Raman spectra zoomed at the wavelength regime from 250 to 320 cm-1. (f) Photoluminescence (PL) spectrum of a $MoSe_2$/PS-NH_2 film on a glass substrate obtained with an excitation laser of 532 nm in wavelength.

The photoelectric properties of the thin nanocomposite film containing $MoSe_2$ nanosheets were examined, and the results are shown in Figure 7. The few-layered $MoSe_2$ nanosheet flakes modified with $PSNH_2$ are closely packed, as shown in the scanning electron microscopy (SEM) image in Figure 7a. The transmission electron microscopy (TEM) images
obtained from the diluted $MoSe_2$ suspension in Figure 7b, c and d confirm a few layer exfoliations of the nanosheets and shows that individual flakes are approximately 5.0 nm in thickness. The Raman spectroscopy results in **Figure 7e** confirm the formation of few-layered

DISTRIBUTION A: Approved for public release; distribution unlimited

MoSe2 nanosheets. The Raman spectrum of the MoSe2/PS-NH2 composite on the SiO2 substrate is compared with that of bulk MoSe2 in **Figure 7e**. The A1g vibration mode of MoSe2 softens in the Raman spectrum of the MoSe2 film, because of weakening of interlayer coupling upon decrease in the number of layers. On the other hand, the E^1_{2g} vibration mode stiffens because of strong dielectric screening of the long-range Coulombic interaction with decrease in the number of layers. Based on the degrees of blue-shift of E^1_{2g} mode and red-shift of A1g mode of the exfoliated MoSe2, we expect that few-layered nanosheets are predominant in the film, which is consistent with the previously reported distribution of number of layers of exfoliated TMD nanosheets. The intensity of the E^1_{2g} peak increased because of the physical repulsion of the MoSe2 flakes arising from the incorporation of PS-NH2. Thus, the Raman spectroscopy results reveal that few-layered MoSe2 nanosheets are dominant in the film, in which the E^1_{2g} and the A1g peaks, corresponding to out-of-plane and in-plane modes, are blue- and red-shifted, respectively, with a frequency difference of approximately 0.4 cm^{-1}. The photoluminescence (PL) spectrum of the MoSe2/PS-NH2 composite on the glass substrate was recorded at an excitation wavelength of 532 nm, and the results are shown in **Figure 7f**. The PL peak centered at approximately 823.0 nm (1.53±0.01 eV), arising from the A excitons of MoSe2, is attributed to an indirect-to-direct bandgap transition which occurs at the K high symmetry point of the Brillouin zone associated with quantum confinement in the perpendicular direction. This implies the presence of substantial amounts of single layered MoSe2 nanosheets in the film prepared on water surface.

5. Conclusions

In the 2nd year research, we have made the progress in understanding molecule-to-molecule and crystal lattice-to-lattice interaction between polymer crystals with hierarchical structures and single or polycrystalline TMDs. First of all, the crystal-to-crystal interaction between polymer and 2D material was studied by examining the epitaxy of polymer crystals on a variety of crystals including organic single crystals, graphene and TMD. Polymer crystals globally ordered with the specific crystal orientations were developed, depending upon the epitaxial relation between polymer and a host crystal. The periodic nano and micron-scale structures of the polymer crystals also systematically investigated under various polymer film thickness and crystallization rate. Secondly, we demonstrated a simple, yet robust supramolecular assembly route for fabricating both vertical and in-plane cylindrical nanostructures globally ordered over a large area with chemical functionalities on their surfaces. Our process is based on solution-blending of two mono-end functionalized polymers with two complementarily interacting end-sulfonate and amine groups. Finally, the series of PS-NH_2 allowed us to reveal the importance of amine-transition metal for the liquid phase exfoliation of TMDs. We fabricated thickness-controlled MoS_2 films consisting of single and few layered nanosheets by liquid exfoliation of bulk $MoSe_2$ with amine-terminated polymers. The liquid exfoliated TMDs can be transferred onto target substrate to fabricate photodetector. The functional materials with full understanding the materials-to-materials interactions will be suitable for high performance applications including, wearable electronics, human performance sensors, and broad band photodetectors.

DISTRIBUTION A: Approved for public release; distribution unlimited

<List of Publications and Significant Collaborations that resulted from your AOARD supported project>

1) Publications

1. “Epitaxially Grown Ferroelectric PVDF-TrFE Film on Shape-Tailored Semiconducting Rubrene Single Crystal”, Small (2018), 14, 1704024

2. “Surface functionalized nanostructures via position registered supramolecular polymer assembly”, Nanoscale (2018), 10, 6333-6342

3. “Flexible Vertical p–n Diode Photodetectors with Thin N-type $MoSe_2$ Films Solution-Processed on Water Surfaces” (2018), 10, 34543–34552

2) Interaction with Air Force

- Setting up future research collaboration in the field of 2D materials and their photo-electronic applications. In particular, research collaboration with Dr. McConney's group on the subject of the electrical characterization of TMD films grown in AFRL as well as epitaxial growth of functional polymers on the TMD films.
- Dr. Richard H. Kim mainly involved with his TMD exfoliation research in the project received the post-doctoral fellowship from AFRL and began to work at Dr. McConney’s group from Jan. 9, 2017.

DISTRIBUTION A: Approved for public release; distribution unlimited